Adv. Polar Upper Atmos. Res., **15**, 146–158, 2001

VLF/LF sounding of the lower ionosphere to study the role of atmospheric oscillations in the lithosphere-ionosphere coupling

O.A. Molchanov[1], M. Hayakawa[2] and K. Miyaki[2]

[1] *Earth Observation Research Center, National Space Development Agency of Japan, Roppongi 1-9-9, Minato-ku, Tokyo 106-0032*
[2] *University of Electro-Communications, Chofugaoka 1-5-1, Chofu-shi, Tokyo 182-8585*

Abstract: It is shown that sounding of the lower ionosphere boundary by subionospheric signals from powerful VLF/LF transmitters can be a useful tool for the investigation of Planetary Waves (PW) with periods in a range of 2–30 days. A specific spring-time transition in the PW dynamic periodograms is revealed from our analysis of several years data using Tsushima, Japan VLF transmitter (10.2 kHz) along the path with length of about 1000 km. Earthquake influence in the periodograms could be sometime recognized as an appearance of specific wavelets. We discuss a possibility of PW transportation from the bottom to the upper atmosphere as modulation of shorter-scale gravity waves (GW) inside the troposphere and subsequent demodulation of the GW at the atmosphere-ionosphere boundary for the explanation of observational results. The existence of modulation due to gravity waves in LF signal amplitude is presented to support the above hypothesis.

1. Introduction

Peculiar periodicities in a range of 5–50 days had been observed in many atmospheric parameters and named as atmospheric waves, planetary waves, intraseasonal atmospheric oscillations or Madden-Julian Oscillations (MJO). The last term was introduced as a tribute to the first papers by Madden and Julian (1971, 1972), who discovered planetary-scale long-term oscillations with the periods of 40–50 days in the zonal wind and surface pressure data at equatorial stations and also short-term oscillations with the period of 5 days. There exist now a large number of observational studies describing the spatial and temporal behavior of the long-term MJO in the pressure and temperature variations, precipitations, sea level variations, etc. Atmospheric oscillations are also envisaged in the measurement of Earth angular moment by the length of day (LOD) precise registrations. Tiwari *et al.* (1994) discovered, in LOD fluctuations, clear spectral maxima near the periods of 27, 13 and 9 days. Quasi 5 and 10 days oscillations were noted even in the lightning activity (Harth *et al.*, 1982). Planetary waves (PW) quasi-line spectrum can be considered as continuation of tide spectrum (periods from about 8 hours to 24 hours) and continuum gravity wave spectrum (periods from 5–7 min to several hours) (Hooke, 1977).

It is usually believed that MJO or PW are normal mode Rossby waves. They are planetary-scale westward propagating features that represent the resonant states of the atmosphere. The basic characteristics of these modes may be mathematically obtained

from the shallow water equations on a rotating global sphere (Longuet-Higgins, 1968). Ceisler and Dickinson (1976) using model of the uniform atmosphere with zonal winds yielded that dominant period of these waves should be 5 days. Calculations produced by Salby (1981) for the nonuniform model of the atmosphere exhibited a variety of eigenperiods, especially 2, 5 and 16 days. Venne (1989) discussed normal Rossby waves at the stratosphere and troposphere with period 4–5, 7–9, and 16 days. Excitation of PW is not clear at present. The simplest approach was developed by Ahlquist (1982) who studied the normal mode response to realistic winds. If so, taking into consideration that regular wind velocities increase up to 70–90 m/s at heights 80–90 km, then the upper atmosphere should be more favorable for the existence of short-term PW with period in a range of 2–10 days.

Indeed, there are a lot of papers on the observation of such oscillations in the upper atmosphere and ionosphere. For example, Wu *et al.* (1993, 1994) observed 2-days and 5-days oscillations at heights 50–110 km by high resolution Doppler radar from satellite. Pancheva *et al.* (1991) found 2–15 days oscillations in the ionospheric absorption, Yi and Chen (1993) discovered 2–2.5, 3–4, 5–7, and 10–18 days oscillations in the equatorial ionospheric ionization and Shimakura *et al.* (1991) found 2 and 4 days variations in the occurrence rate of whistlers.

Recently the HF radar registrations of meteor-induced scattering at heights 85 ± 5 km (so-called meteoradar data) were applied for PW research. It seems, however, that VLF sounding of the same area could also be useful and even more compatible with larger spatial scale of PW taking into consideration the larger VLF wavelength and corresponding increase of sensitivity zone (see the first Fresnel zone in the next section).

VLF signal method is a well-known radiophysical method, in which phase and amplitude of radio signals from navigational transmitters propagating inside the Earth-ionosphere waveguide are monitored. If transmitter frequency and receiver distance are fixed, then the observed VLF signal parameters are mainly dependent upon the reflection height (typically 80–85 km), which depends on the value and gradients of electron density near the atmosphere-ionosphere boundary. Therefore, the VLF signal method has become standard for recording short-time electron density variations in the lower ionosphere and upper atmosphere connected with solar radiation (*e.g.* Roentgen flares), cosmic rays (Forbush effect), precipitation of energetic particles, lightning-induced ionization, ionosphere modification by HF transmitters and, of course, with atmospheric nuclear tests.

Some times ago the VLF signal monitoring was applied for the analysis of long-term variations related to seismic activity. Rather interesting results were obtained in connection with the famous Kobe earthquake and other large earthquakes in Japan (Hayakawa *et al.,* 1996; Molchanov *et al.,* 1998a; Molchanov and Hayakawa, 1998). These authors have suggested the special method of data processing (terminator time (TT) method) and have found a correlation of VLF signal variations with PW activity.

2. VLF signal processing for revelation of long-term trends: TT method

We considered VLF data received at Inubo (near Tokyo) (geographic coordinates: 35°42′N, 140°52′E) and transmitted from 'Omega', Japan (Tsushima, 34°37′N,

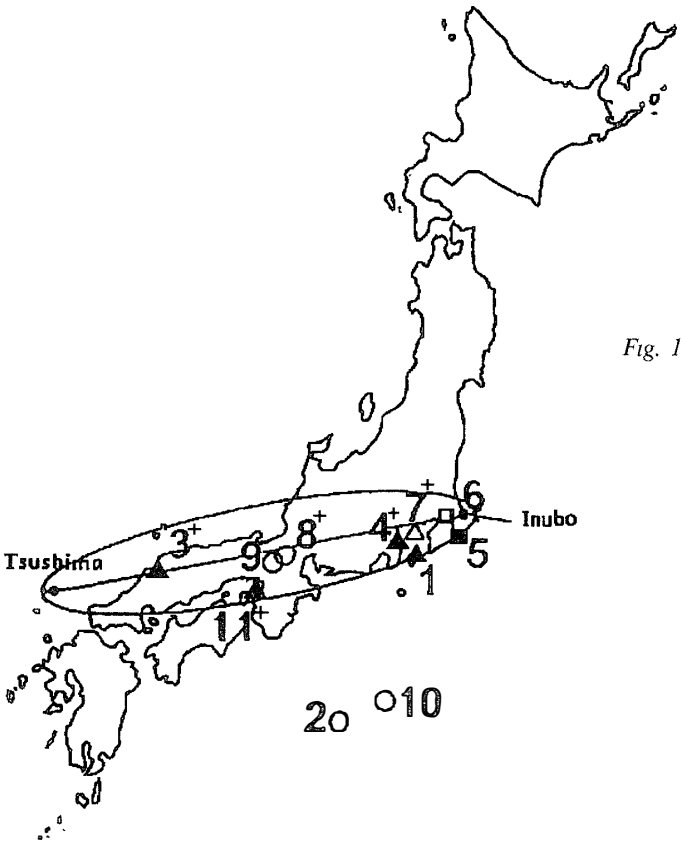

Fig. 1. Location of transmitter (Tsushima, Japan), receiving station (Inubo) and the 1st Fresnel zone are shown. Epicenters of the large earthquakes, for which VLF signal influence is considered in this paper, are indicated by triangles (for crust earthquakes with depth $d<30$ km), squares ($30<d<100$ km) and circles (for deep-focus earthquakes, $d>100$ km). Indicators are black, when correlation of TT variation and earthquake is discovered, and they are white in a case of its absence. Mark "+" near each number shows the case in which spectrum wavelet is found.

129°27′E). The relative location of the transmitter and receiving station is given in Fig. 1, together with the great circle path between them and the first Fresnel zone. The first Fresnel zone is defined as an elliptical area of VLF signal sensitivity to the lower ionosphere perturbations and its minor semiaxis ~100 km, but major axis is about the distance of VLF propagation $D \cong 1054$ km in our case. An example of daily registration at Inubo is shown in Fig. 2. Behavior of the VLF phase and amplitude is rather stable at daytime and is not so stable at nighttime. And there are two minima at the evening and morning time which are called terminator times (abbreviated as TT) (t_e, t_m), which are especially evident for the signal with frequency $f=10.2$ kHz. It was found that monthly-averages of times ($<t_m>$ and $<t_e>$) correlate together with seasonal variations of sunrise and sunset near the end of the VLF path (at Tokyo), so these times are explained by terminator plasma density transition. It was also shown that the differences $\Delta t_{e,m}=t_{e,m}-<t_{e,m}>$ (TT variations) are rather sensitive to the changes in the lower ionosphere boundary height h (Hayakawa *et al.*, 1996; Molchanov *et al.*, 1998a) and there is the following proportionality:

$$\Delta t/\tau_T \approx \Delta h/h, \tag{1}$$

where τ_T is the duration of terminator transition (≈ 2 hours). It could be understood in terms of intensification of the higher VLF signal modes during the move of laterally inhomogeneous terminator region across the propagation path taking into account that higher modes are more vulnerable to the changes of h-value than the dominant, leading mode (Wait, 1964, see also Discussion). The advantage of TT method in comparison

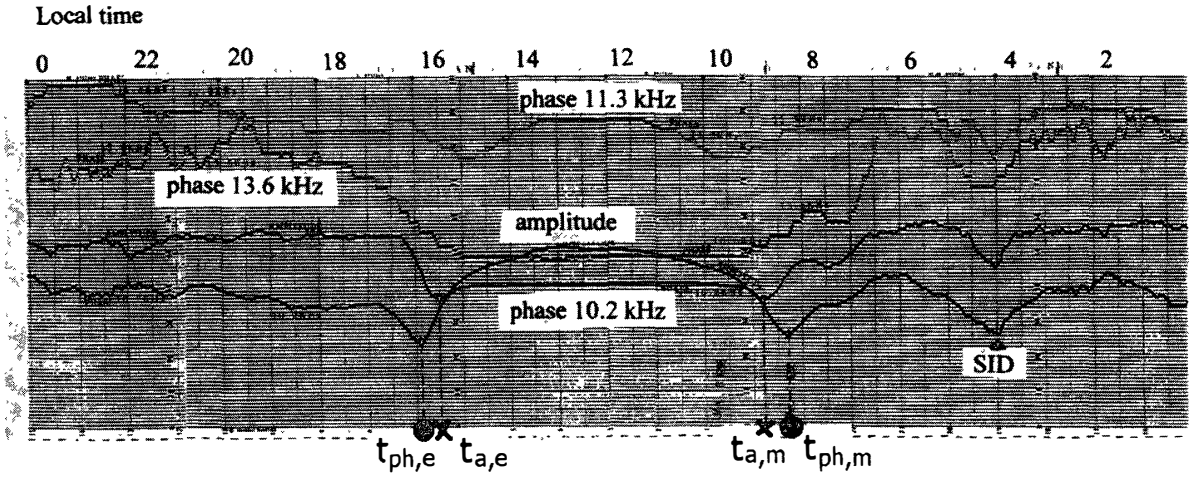

Fig. 2. Example of the usual full-day registration of VLF signals at Inubo station. There are definite minima for 10.2 kHz signal both in phase (shown by dots) and in amplitude variation (crosses). They are connected with terminator changes of electron density profile along the VLF path (see text). Nighttime (at ~4 am) changes of the signals related to sudden ionospheric disturbance are also labeled here.

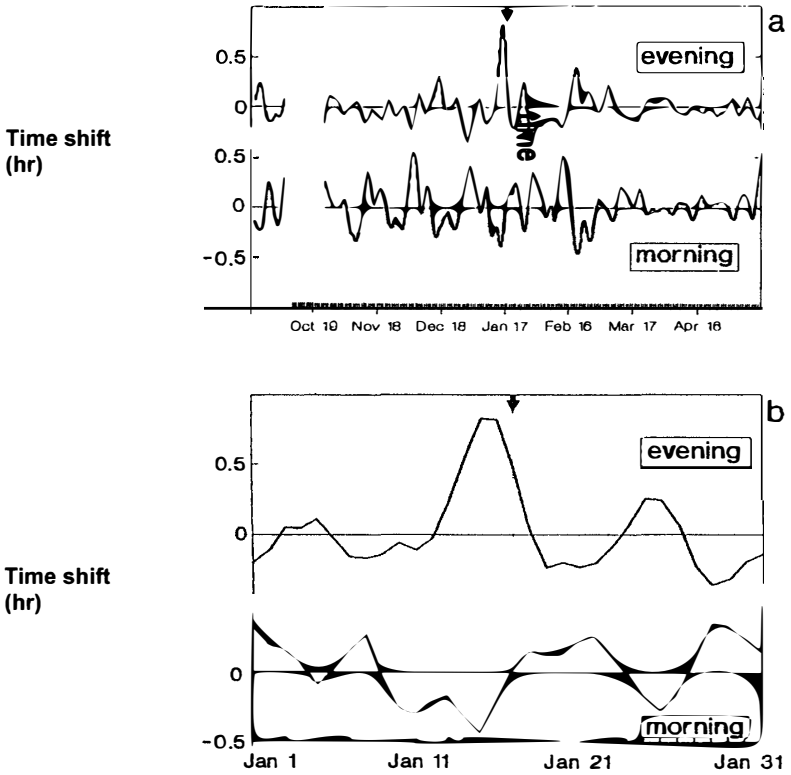

Fig. 3. (a) Comparative variation of phase TT differences at the evening and morning around the date of large Kobe earthquake shown by arrow. (b) The detailed illustration of the change in phase terminator times (evening and morning) for January 1995 only. An enhanced deviation in t_e is observed a few days before the earthquake, with the change in t_m being found to be in opposite phase with that in t_e.

with the conventional analysis of VLF phase and amplitude is obvious. But its disadvantage is that it can be applied only for the analysis of long-term processes with duration of more than 2–3 days. An example of TT variations around the date of Kobe earthquake is presented in Fig. 3. Both quasi-periodic behavior of TT variations and their enhancement near Kobe earthquake date can be easily noticed.

3. Revelation of PW oscillations from VLF data

It is well known that any fluctuations, say $f(t)$, can be characterized by its power spectrum $P_0(F)$, which is introduced in the following manner:

$$<f(t)^2>=\int_0^\infty P_0(F)\mathrm{d}F, \tag{2}$$

where F is frequency of the constitutive oscillation. In the same manner, the distribution of fluctuation energy with oscillation period $\tau=1/F$ can be introduced:

$$<f(t)^2>=\int_0^\infty P(\tau)\mathrm{d}\tau, \tag{3}$$

and the comparison between eqs. (2) and (3) immediately leads to

$$P(\tau)=P_0(1/\tau)\tau^2. \tag{4}$$

It means that the normal spectrum distribution of stochastic fluctuations $P_0(F)\sim F^{-2}\sim\tau^2$ will be flat in the $P(\tau)$ representation. That is why the deviation of $P(\tau)$ from the flat behavior is a signature of nonstochastic processes. In a case of quantization of $f(t)$ during a limited observation period T with sampling rate $(\Delta t)^{-1}$ and the same quantization of oscillation periods $\tau_m=m\Delta\tau$, we can assume,

$$<f(t)^2>=\sum_{m1}^{m2}P(\tau_m)\Delta\tau, \tag{5}$$

where the digital $m1$ and $m2$ are related with sampling rate and T, and $P(\tau_m)$ is averaged energy density in the period window $[(m-1/2)\Delta\tau, (m+1/2)\Delta\tau]$. If $\Delta\tau=\Delta t$ as in our analysis, then $m1=2$ and $m2=T/\Delta t=N$ and it is convenient to use the distribution of relative energy against oscillation period:

$$\varepsilon_m=P(\tau_m)\Delta\tau/<f(t)^2>. \tag{6}$$

First of all, it is a normalized value: $\sum_{m1}^{m2}\varepsilon_m=1$, and furthermore it is easily expressed through Fourier serial coefficients $a(1/\tau_m)=a_m$, $b(1/\tau_m)=b_m$ in the following:

$$\varepsilon_m=2N(a_m^2+b_m^2)/\{(m^2-1/4)(<f^2(t)>-<f>^2)\}. \tag{7}$$

This formula has a limited range of the application, because of an uncertainty in Fourier serial coefficients for $\sqrt{(2N)}<m<N$. However, it is valid if $m\leq m^*=\sqrt{(2N)}$. So, we will calculate ε_m using eq. (7) in a range $m=[2, m^*]$ and call these values as periodogram of VLF signal perturbations or relative distribution of perturbation energy against oscillation period. It is easy to understand now that in our case

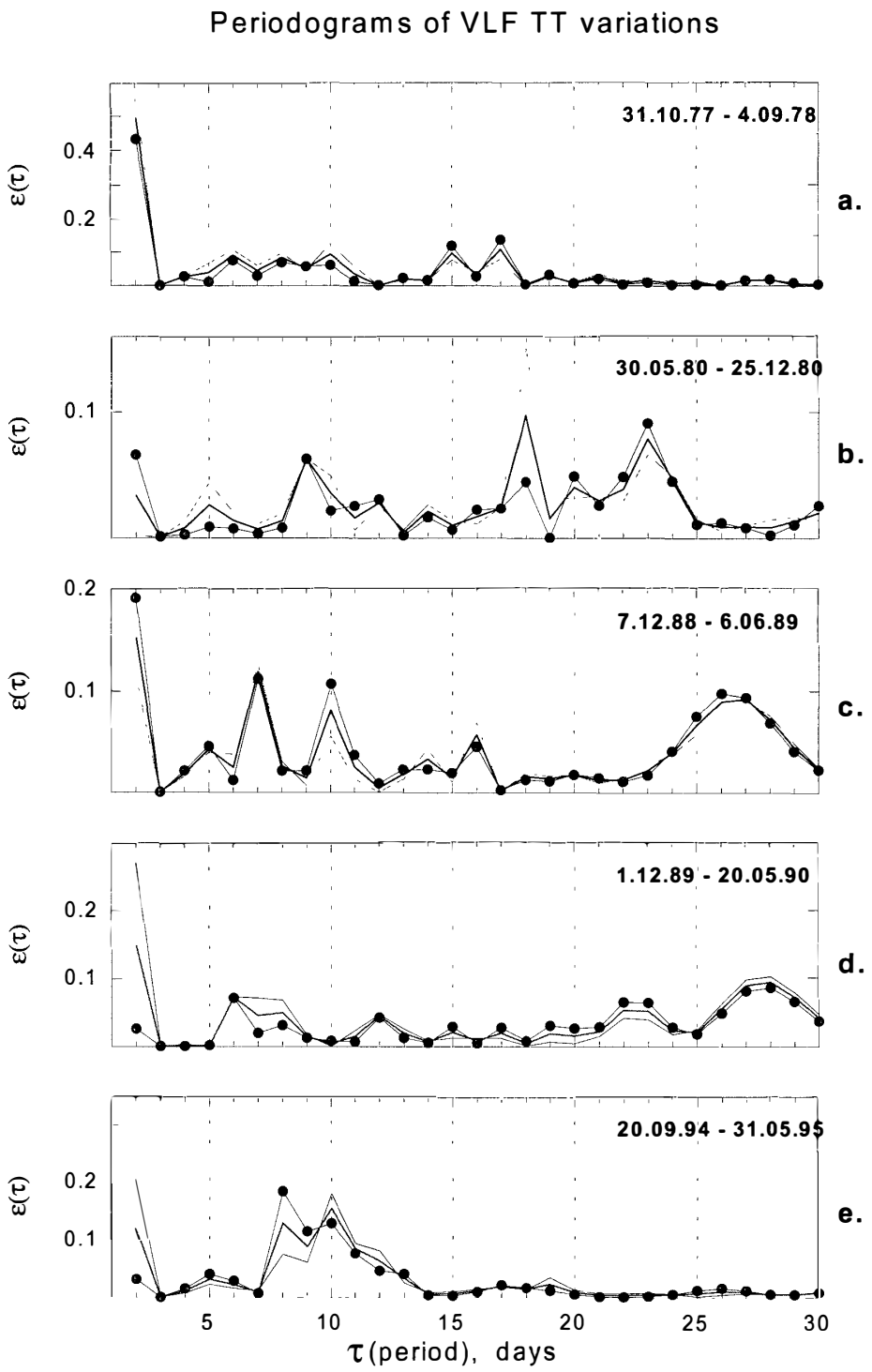

Fig. 4. Peridograms of TT variations during the shown intervals of observation: solid line for the phase, line with dots for the amplitude and thin line is for the average between these values. Almost all the known PW periods are presented here.

$\Delta t = \Delta \tau = 1$ day, m is the period of oscillation in days and N is the number of days in the observation period. If $N = 90\,(365)$, that means 3 months (12 months), then our analysis is valid in a range of periods from 2 days to 14 days (27 days).

Periodograms of VLF signal TT differences are demonstrated in Fig. 4 for the five

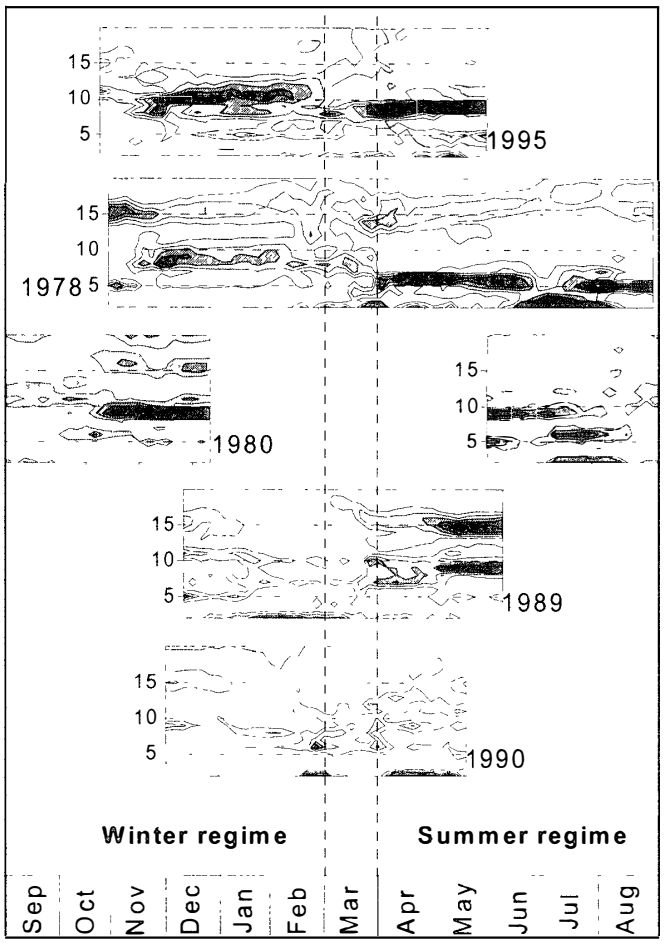

Fig. 5. Seasonal PW activity using dynamic periodograms of VLF TT variations. Isoline factor is 0.3, black filling is for maximum amplitude. Note the change from winter to summer regime through spring time transition period (March).

different intervals of observation. It is evident that all the known PW periods could be recognized in presented TT variations after overwhole averaging.

Evolution of these periodicties can be estimated from dynamic periodograms (running 3-month averaging) and is demonstrated in Fig. 5. At least two peculiarities of the PW evolution seem to be noted:

- There are two definite regimes of PW occurrence. Winter regime (from about September to February) is characterized by mainly the periods of 9–11 days and 15–16 days. 2-days and 5-days PW periods are weak or absent. Appearance of strong 2, 5-days oscillations in February 1990 is an exceptional case which will be discussed in the next section. In contrast, summer regime (from about April to August) is richer in the PW activity and rather strong oscillations with periods 2–3 days, 5–6 days, 9–10 days and 15–16 days took place.
- Clear springtime transition from winter to summer regime during March is evident. The similar autumn-time transition is not envisaged due to the lack of data (only one interval of registration in 1980 contains September time), but it can be supposed.

4. Possible seismic influence from PW behavior

We discovered convincing seismic signatures in TT variations, duration 10–20 days, for several large earthquakes, with their positions being shown in Fig. 1. They are

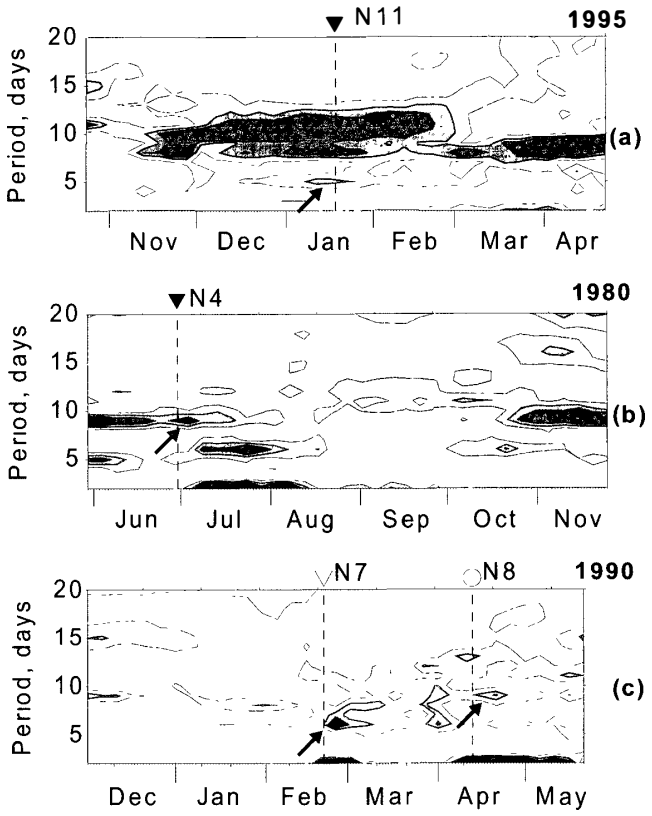

Fig. 6. Dynamic periodograms for three intervals of observation with indication of earthquake (EQ) moments (their positions are depicted in Fig. 1). PW wavelets are possibly associated with the earthquakes shown by arrows. a) Time difference between center of the wavelet and moment of EQ N11, $\Delta t = -3$–4 days. It is nearly the same as for corresponding TT variations (see Fig. 3). b) $\Delta t \approx +5$ days for EQ N4. c) $\Delta t = +6$ days for EQ N7 and $\Delta t \approx +7$ days for EQ N8.

similar to that depicted in Fig. 3 and have appeared mainly for the crust earthquakes (source depth less than 30-km, see the paper by Molchanov and Hayakawa, 1998). The mechanisms of such an influence are not so clear now and we have suggested near-ground atmospheric wave intensification which is probable during the earthquake process about ± 1–2 weeks around the date of main shock. Our arguments were based on the analysis of dynamic periodograms. Three examples are presented in Fig. 6.

In Fig. 6a we can see an appearance of wavelet in 5-day period PW just around the date of Kobe earthquake (January 17, 1995, magnitude $M = 7.2$). Its duration is about 3 weeks and it is not so usual for the winter regime of PW (see above). So, it can be supposed as being related to the earthquake. The similar wavelet, but with 9-day period, can be assumed around the date of earthquake N4 (June 29, 1980, $M = 6.7$) in Fig. 6b. But the most interesting case is demonstrated in Fig. 6c. It is appearance of two wavelets with periods 2-days and 6-days near the date of earthquake N7 (February 20, 1990, $M = 6.5$). It is only a crust earthquake for which we could not find any significant change in TT variations (see Fig. 1 and the paper by Molchanov and Hayakawa, 1998). The 6-days wavelet is a little delayed in comparison with the previous ones. As concerned with 9-day wavelet near the date of earthquake N8 (April 12, 1999, $M = 6.4$), it also happened after the main shock and its connection with the earthquake is not so probable as for the previous cases.

If wavelets showed are associated to seismic perturbations indeed, then the main problem of possible explanation is time delay between the climax of earthquake process (moment of main shock) and the time of wavelet center. This visible delay is several days. However, the matter is that upward transport of PW energy is very slow

(theoretical group velocity less than 0.05 m/s) and expected transport time from the bottom of atmosphere into the lower ionosphere is more than 20–30 days. So we need to suppose that PW oscillations are coupled with a faster carrier wave, for example gravity wave (GW). It is possible when we take into account nonlinearity of equations describing the atmosphere processes. Let us consider for simplicity that some amplitude-modulated gravity waves have appeared in the troposphere with the following temporal dependence of density variation:

$$N_t(t) = (u_{gt} + A_{tm} \sin(\Omega_m t)) \sin(\omega_g t + \phi(z, t)), \tag{8}$$

where u_{gt} is the amplitude of tropospheric GW (frequency ω_g) and A_{tm} is the amplitude of PW in the troposphere (frequency Ω_m). If GW wavelength is of the order of 100–300 km that is comparable with the size of seismic perturbation above an epicenter, then GW periods are of the order of 20 minutes-1 hour and their transport time into the lower ionosphere region is about 1 day or so. Decoupling in the upper atmosphere is also possible. In a case of quadratic nonlinearity the resultant amplitude of slow oscillation at the ionosphere boundary will be the following:

$$N_b = \alpha(u_{gt} A_{tm} \sin(\Omega_m t) + 1/2 A^2_{tm} \sin(2\Omega_m t)), \tag{9}$$

where α is the coefficient of nonlinear transformation. Assuming a decrease in height

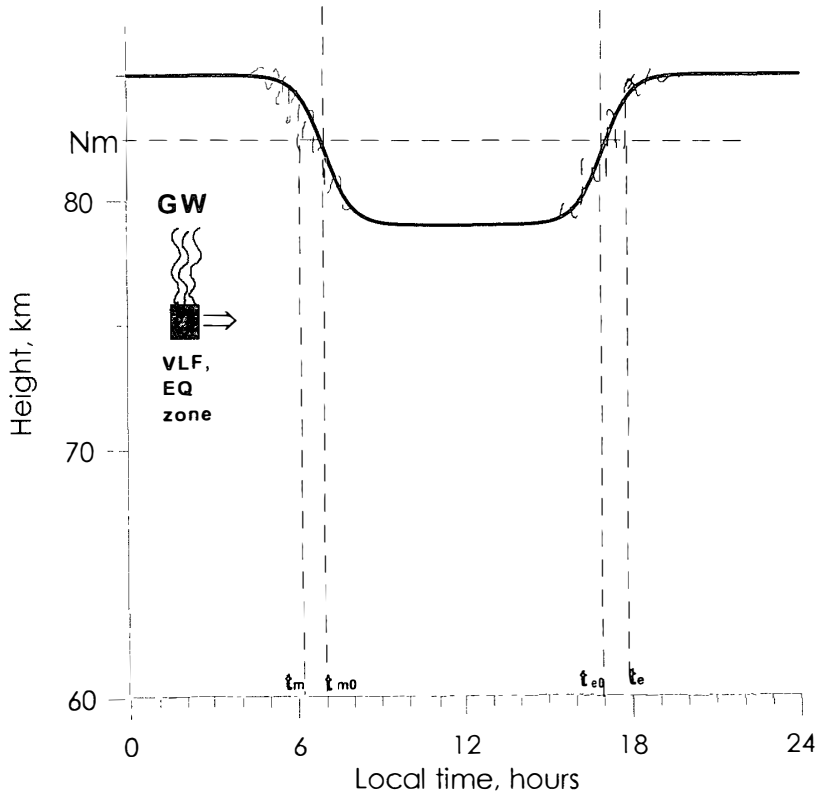

Fig. 7. Scheme of GW influence on VLF signal at the terminator area. Relative movement of perturbation zone and the terminator structure is shown by arrow. Dependence of reflection height on local time is pictured by solid line (regular situation) and by dashed line in a case of perturbation (see text).

of PW generation with period $\tau_m = 2\pi/\Omega_m$ and $u_{gt} \geq A_{tm}$ we have finally:

$$\varepsilon_m \approx u^2_{gt} A_{tm}^2 / \Sigma (N_{bi}^2), \tag{10}$$

where the sum in the denominator is fulfilled over the power of all the PW oscillations (i: PW component) generated both in the troposphere and stratosphere. Thus PW intensity at the lower ionosphere could be correlated with gravity wave intensity near the ground influenced by seismic activity even if the tropospheric PW oscillations do not expose to such an influence at all.

Let us try now to understand the anti-phase behavior of TT-variations shown in Fig. 3. It can be done on the same suggestion of earthquake-associated GW perturbation with horizontal scale 100–300 km and an additional assumption that these GWs may be stimulated by an unstable state of plasma at the height about 80 km during the terminator transition time. The situation is depicted in Fig. 7. Full scale of terminator zone is about 2000–3000 km and it is moving over the position of VLF path and the place of GW generation which is inside the sensitivity zone (scale about 1000 km). The latitudinal path is supposed that is valid in our case (see Fig. 1). Roughly speaking the interference minimum corresponds to a definite value of electron density (N_m in Fig. 7). So, it is evident that appearance of density inhomogeneity, triggered by GWs during the course of passing terminator zone just above the epicentral area, leads to a shift in morning terminator minimum ahead and it leads to a delay in the evening TT. It is exactly what has been observed.

5. Evidence of GWs related with seismic activity

The most serious problem in the previous section is the assumption of existence of seismic-associated GWs. In order to investigate this problem, we have used the data observed at Chofu for the subionospheric signal from a LF transmitter (JG2AS) located at Fukushima prefecture (frequency = 40 kHz, power = 10 kW). The distance between the transmitter and receiver is about 220 km, so that the sky wave is a little stronger than the ground wave at Chofu. The amplitude and phase of that subionspheric LF signal are continuously recorded at Chofu, but we have used only the amplitude data. The

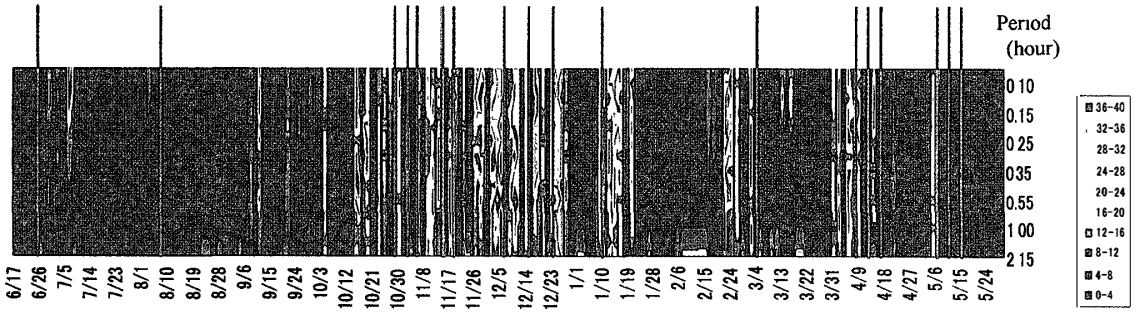

Fig. 8. Temporal evolution of fluctuation spectra in the frequency range of gravity wave (6 minutes to 2.15 hours) in the LF amplitude data observed at Chofu. Daytime, 0900–1314 LT during the period of June 17, 1999 to May 31, 2000. Fluctuation power is given in color code, and the vertical lines indicate the time of earthquakes within the 3rd Fresnel zone and with magnitude greater than 4.0.

data used for the analysis of fluctuation spectra are taken not only at day (0900–1314 LT) but also at night (2152–0216 LT). This four hours interval was selected in order to be free from the seasonal variation of terminator times. The way of analysis is exactly the same as the periodogram in the previous section. Figure 8 is the one-year result in the period range of GW from about 10 min to ~2 hours only for daytime at Chofu. The vertical lines indicate the time of earthquakes which take place within the 3rd Fresnel zone and whose magnitude is greater than 4.0. The figure shows that there are significant enhancements in the fluctuation power in the period range of GWs during the period from the middle October 1999 to January 2, 2000, when we had enhanced seismic activity. Then we have a quiet period up to the middle February 2000, and again there is observed an increase in fluctuation spectra for about ten days before the quake on March 4, 2000. As seen from this figure, it is likely that the modulation in amplitude with period of GWs is seen, at least, just around the quake. This result may not deny the important role of GWs as our important hypothesis in the previous section.

6. Discussion

Scope and targets of this paper do not suppose any extended theoretical discussion. But several of rather speculative aspects seem to be at least briefly mentioned. The first is the high sensitivity of our TT method. Using the classical approach to VLF wave propagation by expansion of the wave in terms of modal waves (*e.g.* Wait, 1964) it can be shown that relationship between the variation of modal phases and amplitudes ϕ_n, u_n (n is number of mode) and the variation of efficient reflection height h is as follows:

$$\begin{aligned} \Delta\phi_n/2\pi &\approx \lambda D/(4a_n h^2)(\Delta h/h)n^2, \\ \Delta u_n/u_n &\approx a_n(\lambda^2/4h^2)(\Delta h/h)n^2, \end{aligned} \tag{11}$$

where $a_n = Re\ (S_n)$, S_n is complex sine depending mainly on λ, h, and n (see Wait, 1964) and λ is VLF wavelength ($\lambda = 29.4$ km in our case). Modal interference during the terminator transition depends on many factors. First, it depends on the phase of the leading mode ($n = 1$ in our case). It is envisaged in Fig. 2: the signal with $f = 11.3$ kHz shows a weak terminator minimum and the signal with $f = 13.6$ kHz does not exhibit any. Then the interference depends on the evolution of electron density profile: change in phase and amplitude of the signal with $f = 10.2$ kHz is more definite for the evening terminator than for the morning one (it was a reason why we discussed mainly the results of evening TT). There is also dependence on number of modes efficiently involved in the modal superposition n_0; supposing that all the propagating modes ($n \leq 5$) could be intensified. In the favorite situation the estimation relationship like eq. (1) is the following:

$$\Delta t/\tau_T = b(\lambda L/h^2)n_0^2(\Delta h/h), \tag{12}$$

where b is a constant of the order of 1 and L is the common size of terminator and sensitivity zones ($L \sim D$ in our case). Hayakawa *et al.* (1996) used a very simple simulation model assuming a smooth profile of terminator transition and corresponding suppression of higher modes in comparison with the leading one. It means $n_0 \sim 1$ and from their computations $b \approx 7$. It leads to maximal values of $\Delta h_m \approx 2$ km for observed

$\Delta t/\tau_T \approx 1/3$. But if we suppose an inhomogeneous profile of terminator transition zone (like depicted in Fig. 7) and corresponding intensification of higher modes, then we need to use in eq. (12) $n_0 \sim 3$–4. It yields to variation $\Delta h/h \leq 0.01$ that seems as reasonable.

Another approach is consideration of propagation near the terminator as scattering. This approach showed an efficiency for the investigation of so-called Trimpi effect (see *e.g.* Molchanov *et al.,* 1998b and references therein). However, using both types of consideration we need to assume that the perturbation area is not very far from the receiving station (≤ 800 km) in order either to keep multi-modal structure or to receive efficiently the scattering signal.

We supposed an essential coupling between PW and GW both in the troposphere and lower ionosphere. Recently rather strong coupling between 2-day PW oscillations and tides was demonstrated (Palo, 2000). We then assumed a possibility of electron density irregularities at the lower ionosphere triggered by GWs in the unstable terminator area. This idea does not seem to be so speculative, remembering that possibility of initiation of large-scale irregularities in the quasi-stable near-equatorial anomaly at E-layer by "seeding" GWs is a well-discussed problem of the ionospheric physics (*e.g.* Huang and Kelley, 1996).

In conclusion, we have tried to show that VLF sounding of the atmosphere-ionosphere boundary is a rather useful method for the investigation of atmospheric large-scale waves and especially for revelation of such a weak source as lithospheric seismicity.

Acknowledgments

We are grateful to Ms. L.Ya. Tourivnenko for her help in preparation of this paper.

The editor thanks Dr. M. Parrot and another referee for their help in evaluating this paper.

References

Ahlquist, J.E. (1982): Normal-mode global Rossby waves. J. Atmos. Sci., **39**, 193–202.

Ceisler, J.E. and Dickinson, R.E. (1976): The five-day wave on a sphere with realistic zonal winds. J. Atmos. Sci., **33**, 633–641.

Harth, W., Steffen, P., Hofman, C.A. and Falcos, A. (1982): The day-to-day variation of atmospherics activity over the South American continent. J. Atmos. Terr. Phys., **44**, 121–129.

Hayakawa, M., Molchanov, O.A., Ondoh, T. and Kawai, E. (1996): Anomalies in the sub-ionospheric VLF signals for the 1995 Hyogo-ken Nanbu earthquake. J. Phys. Earth, **44**, 413–418.

Hooke, W.H. (1977): Rossby-planetary waves, tides, and gravity waves in the upper atmosphere. The Upper Atmosphere and Magnetosphere, Studies in Geophysics, Washington, Nat'l Acad. Sci., 130.

Huang, C.S. and Kelley, M.C. (1996): Nonlinear evolution of equatorial spread F, 1, On the role of plasma instabilities and spatial resonance associated with gravity wave seeding. J. Geophys. Res., **101**, 283–292.

Longuet-Higgins, M.S. (1968): The eigenfunctions of Laplace's tidal equations over a sphere. Philos. Trans. R. Soc., London, **262A**, 511–607.

Madden, R.A. and Julian, P.R. (1971): Detection of 40–50 day oscillation in the zonal wind in the tropical Pacific. J. Atmos. Sci., **28**, 702–708.

Madden, R.A. and Julian, P.R. (1972): Further evidence of global-scale 5-days pressure waves. J. Atmos. Sci.,

29, 1464–1469.

Molchanov, O.A. and Hayakawa, M. (1998): Subionospheric VLF signal perturbations possibly related to earthquakes. J. Geophys. Res., **103**, 17489–17504.

Molchanov, O.A., Hayakawa, M., Ondoh, T. and Kawai, E. (1998a): Precursory effects in the subionospheric VLF signals for the Kobe earthquake. Phys. Earth Planet. Inter., **105**, 239–248.

Molchanov, O.A., Shvets, A.V. and Hayakawa, M. (1998b): Analysis of lightning-induced ionization from VLF Trimpi events. J. Geophys. Res., **103**, 23443–23458.

Palo, S.E. (2000): Nonlinear interaction between the quasi-two-day wave and the migrating tides in the middle atmosphere. Abstracts of Int'l Workshop on Atmospheric Oscillations, Prague, Czech.

Pancheva, D., Lastovichka, Y. and Morena, B.A. de la (1991): Quasi-periodic fluctuations in ionospheric absorption in relation to planetary activity in the stratosphere. J. Atmos. Terr. Phys., **53**, 1151 -1155.

Salby, M.L. (1981): Rossby modal models in nonuniform background configurations. J. Atmos. Sci., **38**, 1803–1840.

Shimakura, S., Yamamoto, T. and Hayakawa, M. (1991): On the short and long periodicities in whistler occurrence rate and their implication. Res. Lett. Atmos. Electr., **11**, 23–36.

Tiwari, R.K., Negi, J.G. and Rao, K.N.N. (1994): Strange attractor in nonlinear fluctuations of the length of the day(LOD) time series. Nonlinear Dynamics and Predictability of Geophysical Phenomena, ed. by W.I. Newman *et al.* Geophys. Monograph, **83**, 61–68.

Venne, D.E. (1989): Normal-mode Rossby waves observed in the wavenumber 1-5 geopotential fields of the stratosphere and troposphere. J. Atmos. Sci., **46**, 1042–1055.

Wait, J.R. (1964): Electromagnetic Waves in Stratified Media. Tarry town, Pergamon.

Wu, D.L., Hays, P.B., Skinner, W.R., Marshall, A.R., Burrage, M.D., Lieberman, R.S. and Ortland, D.A. (1993): Observation of the quasi 2-days wave from the High Resolution Doppler Imager on UARS. Geophys. Res. Lett., **20**, 2853–2856.

Wu, D.L., Hays, P.B. and Skinner, W.R. (1994): Observations of the 5-days wave in the mesosphere and lower thermosphere. Geophys. Res. Lett., **21**, 2733–2736.

Yi, L. and Chen, P.R. (1993): Long period oscillations in the equatorial ionization anomaly correlated with the neutral wind in the mesosphere. J. Atmos. Terr. Phys., **55**, 1317–1323.

(Received December 5, 2000; Revised manuscript accepted April 5, 2001)